Implication of the tRNA Initiation Step for Human Immunodeficiency Virus Type 1 Reverse Transcriptase in the Mechanism of 3‘-Azido-3‘-deoxythymidine (AZT) Resistance †

ARTICLE *in* BIOCHEMISTRY · NOVEMBER 1998

Impact Factor: 3.02 · DOI: 10.1021/bi9810353 · Source: PubMed

2 AUTHORS, INCLUDING:

Karen S Anderson
Yale University
194 PUBLICATIONS **5,759** CITATIONS

SEE PROFILE

Implication of the tRNA Initiation Step for Human Immunodeficiency Virus Type 1 Reverse Transcriptase in the Mechanism of 3′-Azido-3′-deoxythymidine (AZT) Resistance†

Joseph A. Vaccaro and Karen S. Anderson*

Department of Pharmacology, Yale University School of Medicine, 333 Cedar Street, New Haven, Connecticut 06520-8066

Received May 5, 1998; Revised Manuscript Received July 24, 1998

ABSTRACT: There is a lack of correlation between biochemical studies and the observed clinical resistance of AIDS patients on long-term AZT therapy. Mutant HIV-1 reverse transcriptase in the viral isolates from these patients shows a 100-fold decrease in sensitivity to AZT whereas little or no difference is observed in kinetic parameters *in vitro* using steady-state kinetic analysis. A pre-steady-state kinetic analysis was used to examine the binding and incorporation of 2′-deoxythymidine 5′-triphosphate (dTTP) and 3′-azido-3′-deoxythymidine 5′-triphosphate (AZTTP) by wild-type HIV-1 reverse transcriptase and a clinically important AZT-resistant mutant form of the enzyme (D67N, K70R, T215Y, K219Q) utilizing a physiologically relevant RNA 18-mer/RNA 36-mer primer-template substrate. It was determined that with this RNA/RNA substrate there is a 2.6-fold increase in the selection for incorporation of the natural nucleotide dTTP over the unnatural nucleoside analogue AZTTP by AZT-resistant reverse transcriptase as compared to its wild-type form. This observation indicates that the $tRNA^{Lys}$ initiation step plays an important role in the development of drug resistance. Furthermore, this result implies that the structural basis of AZT resistance in HIV-1 reverse transcriptase involves the conformation of the RNA−DNA junction (formed upon attachment of a deoxynucleotide to the RNA primer). Taken together, these observations suggest a new pharmacological basis for the development of more effective and novel AIDS drugs.

Virally-encoded human immunodeficiency virus (HIV)[1] reverse transcriptase (RT) catalyzes the conversion of the single-stranded viral RNA genome to a double-stranded DNA copy that is subsequently integrated into the host cell DNA. RT is an enzyme with unique catalytic properties in that it must first catalyze the initiation of DNA synthesis from an RNA/RNA primer-template duplex in which the human $tRNA^{Lys}$ serves as a primer on the RNA genome. To ultimately form the double-stranded DNA, RT must also catalyze both RNA-dependent and DNA-dependent DNA polymerization in the elongation steps as well as RNase H cleavage to remove the RNA template once the DNA has been synthesized.

RT has been the target of several antiviral therapeutic agents used in the treatment of AIDS (*1*−*3*). Nucleoside analogues such as AZT (3′-azido-3′-deoxythymidine) have been the drugs of choice to inhibit viral replication. However, their long-term use is limited by toxicity (*4*, *5*) and the high frequency of viral mutation whereby drug-resistant forms of RT may accumulate (*6*). The mutations in HIV-1 RT which frequently have been found in clinical isolates to be associated with AZT resistance are in amino acid residues 67, 70, 215, and 219 (*7*−*9*). A fifth mutation in residue 41 conferring a slightly higher level of resistance has also been observed (*10*). The three-dimensional structure of RT is similar to other polymerases in that the overall fold of the protein resembles a right hand with fingers, palm, and thumb domains (*11*−*13*). The palm domain contains the two conserved Asp residues, 185 and 186, which are essential for catalysis. Based on the three-dimensional structure of RT, the mutations that confer AZT resistance map to regions in the fingers and palm domains but are not located at the active site. The mechanism by which RT develops resistance to AZT remains unclear as there is a lack of correlation between the decrease in sensitivity to AZT for AZT-resistant (AZT^R) virus in culture and the *in vitro* evaluation of wild-type and AZT^R RT using steady-state kinetic analysis (*14*−*16*).

Steady-state kinetic analysis is limited by the fact that it reflects the rate-limiting step in the overall reaction pathway. On the other hand, pre-steady-state kinetic analysis allows one to examine each of the individual steps in the pathway including the identification of enzyme intermediates and conformational changes which might be associated with

† This work was supported by NIH Grant GM49551 to K.S.A. and ACS Postdoctoral Fellowship PF-4478 to J.A.V.

* To whom correspondence should be addressed at the Department of Pharmacology, Yale University School of Medicine, 333 Cedar St., New Haven, CT 06520-8066. Phone: 203-785-4526. Email: karen.anderson@yale.edu.

[1] Abbreviations: AIDS, acquired immunodeficiency syndrome; ATP, adenosine 5′-triphosphate; AZT, 3′-azido-3′-deoxythymidine; AZT^R, AZT-resistant; AZTMP, AZT 5′-monophosphate; AZTTP, AZT 5′-triphosphate; dCMP, 2′-deoxycytidine 5′-monophosphate; dCTP, 2′-deoxycytidine 5′-triphosphate; dNTP, 2′-deoxynucleoside 5′-triphosphate; dTMP, 2′-deoxythymidine 5′-monophosphate; dTTP, 2′-deoxythymidine 5′-triphosphate; EDTA, (ethylenediamine)tetraacetate; HIV-1, human immunodeficiency virus type 1; PBS, primer binding site; RT, reverse transcriptase; Tris, tris(hydroxymethyl)aminomethane; WT, wild type.

S0006-2960(98)01035-6 CCC: $15.00
Published on Web 09/15/1998

chemical catalysis (*17*−*20*). Our laboratory (*21*−*23*) and others (*24*−*26*) have used a pre-steady-state kinetic analysis to establish the reaction pathway for RT. The reaction pathway is ordered. The first step involves the binding of the DNA (or RNA) substrate to the enzyme to form a tight E•DNA complex with a K_d value in the nanomolar range. This step is followed by the binding of the correct nucleoside triphosphate. The enzyme checks for proper base-pairing geometry and then undergoes a rate-determining conformational change which limits chemical catalysis. The slowest step in the pathway involves the dissociation of the elongated DNA substrate from the enzyme and is the step which is being examined in a steady-state kinetic analysis (*27*).

We have recently used a pre-steady-state kinetic analysis to examine wild-type and the quadruple mutant AZT^R form of RT in an effort to understand the mechanistic basis of AZT resistance (*28*). This type of analysis has also been used by other laboratories to examine a mutant form of RT which contains the additional fifth mutation at residue 41 (*29*). Each of these studies focused on the elongation phase (DNA/DNA or DNA/RNA) of viral replication. The studies with the mutant form of RT containing five mutations showed little kinetic differences from wild type when using DNA/DNA and DNA/RNA primer-template substrates (*29*). However, studies from our laboratory using the quadruple AZT^R form of RT revealed a 1.5-fold decrease in the maximum rate constant for polymerization (k_{pol}) and a 2.5-fold decrease in the equilibrium dissociation constant (K_d) for AZTTP for a DNA/RNA substrate, indicating that RNA-dependent DNA replication in the elongation step may play a role in AZT resistance (*28*). This small but significant decrease in sensitivity to AZTTP by mutant RT compared to wild-type RT for a DNA/RNA primer-template, however, does not fully account for the 100-fold decrease in sensitivity of AZT observed in the clinic and in cell culture studies. The present study was designed to address the question of whether other parts of viral replication such as the tRNA^{Lys} initiation step may also play an important role in the development of drug resistance.

EXPERIMENTAL PROCEDURES

Materials. All chemicals were of analytical or reagent grade and were used without further purification. All water was prepared on a Milli-Q UF Plus Water System including a $QPAK_2$ purification pack (Millipore). AZTTP was obtained from Moravek Biochemicals, and dCTP and dTTP were purchased from Pharmacia Biotech. [γ-^{32}P]ATP was obtained from Amersham. The 18-mer RNA primer and the 36-mer RNA template were synthesized by New England BioLabs. Both wild-type and AZT^R (D67N, K70R, T215Y, K219Q) HIV-1 RT were purified as previously described (*21, 28*).

General Methods. The concentrations of the RNA oligomers were determined spectrophotometrically at 260 nm using the calculated extinction coefficients $\epsilon_{260} = 177\,000$ M^{-1} cm^{-1} and $\epsilon_{260} = 396\,000$ M^{-1} cm^{-1} for the 18-mer and 36-mer, respectively. The RNAs were 5′-labeled with T4 polynucleotide kinase (New England BioLabs) and [γ-^{32}P]-ATP. The 18-mer/36-mer RNA homoduplex was annealed by incubating a 1:1.4 molar ratio of 18-mer primer (68 Ci $mmol^{-1}$) to 36-mer template (48 Ci $mmol^{-1}$) in 50 mM Tris-HCl (pH 7.8) buffer containing 50 mM NaCl at 90 °C for 3 min and 50 °C for 10 min.

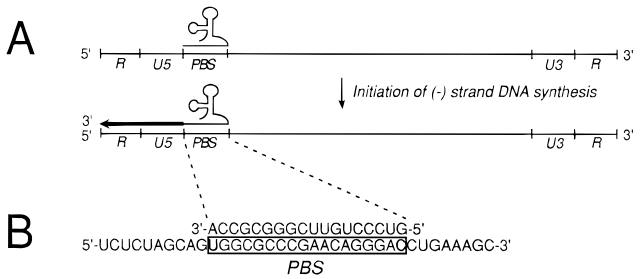

FIGURE 1: Initiation of (−) strand DNA synthesis by HIV-1 RT. (A) HIV-1 RT initiates *in vivo* DNA synthesis from a primer-template complex in which the 18 nucleotides at the 3′ end of a human lysyl tRNA primer are annealed to the primer binding site (PBS) of the HIV genomic RNA template. (B) The primer-template complex used in these studies consists of (*i*) an 18-nucleotide RNA primer whose sequence is identical to the 3′ end of the human lysyl tRNA and (*ii*) a 36-nucleotide RNA template whose sequence is identical to the HIV genome and which contains the PBS sequence (boxed).

The protein concentration of purified RT was measured spectrophotometrically at 280 nm using an extinction coefficient $\epsilon_{280} = 260\,450$ M^{-1} cm^{-1}. The concentration of active RT was determined as previously described with pre-steady-state burst experiments (*21*) that gave burst amplitudes of 40% for both wild-type and AZT-resistant RT, and all enzyme concentrations reported in this study have been corrected using this fraction of active enzyme.

Rapid chemical quench experiments were performed as previously described with a KinTek Instruments Model RQF-3 rapid-quench-flow apparatus thermostated at 37 °C (*21, 28*). Wild-type or AZT^R RT (250 nM active sites) and the doubly 5′-^{32}P-labeled 18/36-mer RNA duplex (50 nM) were preincubated on ice for 5 min in buffer [50 mM Tris-HCl (pH 7.8), 50 mM NaCl]. Polymerization was initiated at 37 °C by the rapid addition of either dCTP alone (1−2000 μM) or 2 mM dCTP and dTTP (50−2000 μM) or AZTTP (68−2000 μM) in buffer containing 10 mM $MgCl_2$, and the reactions were quenched at the indicated times with 0.3 M EDTA. Products were analyzed on a 20% polyacrylamide gel containing 7.5 M urea and 12% formamide followed by phosphorimaging analysis on a BioRad GS-525 Molecular Imager System.

Data Analyses. The data were fit by nonlinear regression using the program SigmaPlot version 4.14 (Jandel Scientific). The data from the single-turnover experiments were fit to a single-exponential equation: [19- or 20-mer] = $A(1 - e^{-k_{obsd}t})$, where A is the amplitude and k_{obsd} is the observed first-order rate constant for dNTP incorporation. The binding curves were fit to the following hyperbolic equation: $k_{obsd} = k_{pol}[dNTP]/(K_d + [dNTP])$, where k_{pol} is the maximum first-order rate constant for dNTP incorporation and K_d is the equilibrium dissociation constant.

RESULTS AND DISCUSSION

The tRNA^{Lys} initiation step involved in the formation of the (−) strand DNA entails the initiation of DNA synthesis using an RNA/RNA duplex in which the 3′ end of the human tRNA^{Lys} anneals to an 18-nucleotide region on the HIV-1 RNA genome known as the primer binding site (PBS) as illustrated in Figure 1A. As a first approach to studying the

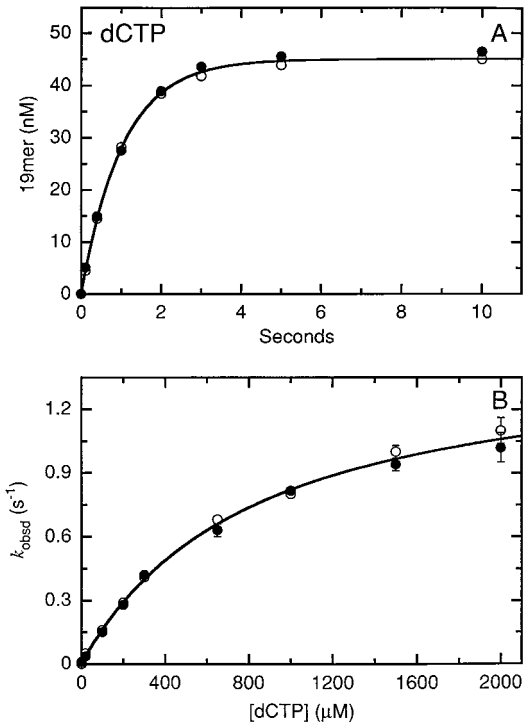

FIGURE 2: Single-turnover dCMP incorporation kinetics and dCTP concentration dependency for wild-type and AZT^R HIV-1 RT. (A) The incorporation of dCMP (1.5 mM dCTP) into the 18/36-mer RNA duplex (50 nM) by wild-type (●) and AZT^R (○) HIV-1 RT (250 nM active sites) was determined at 37 °C in buffer containing 10 mM $MgCl_2$. The time courses for dCMP incorporation by wild-type and AZT^R HIV-1 RT were fit to a single-exponential equation as described, and the curve is drawn for an amplitude $A = 45$ nM and an observed first-order rate constant $k_{obsd} = 0.97$ s^{-1} for both wild-type and AZT^R HIV-1 RT. Note that for the purpose of presentation, these values represent an average of the actual individual values: $A = 46 \pm 1$ nM and $k_{obsd} = 0.94 \pm 0.03$ s^{-1} for wild-type (●) and $A = 44 \pm 1$ nM and $k_{obsd} = 1.00 \pm 0.03$ s^{-1} for AZT^R (○) HIV-1 RT. (B) The dependence of k_{obsd} for incorporation of dCMP into the 18/36-mer RNA duplex (50 nM) by wild-type (●) and AZT^R (○) HIV-1 RT (250 nM active sites) on the concentration of dCTP (1−2000 μM) was determined at 37 °C in buffer containing 10 mM $MgCl_2$. The dCTP concentration dependence of k_{obsd} for wild-type and AZT^R HIV-1 RT was fit to a hyperbolic equation as described, and the curve shown represents a fit for an equilibrium dissociation constant $K_d = 830$ μM and a maximum rate constant for incorporation $k_{pol} = 1.5$ s^{-1} for both wild-type and AZT^R HIV-1 RT. Note that for the purpose of presentation, these values represent an average of the actual individual values: $K_d = 780 \pm 50$ μM and $k_{pol} = 1.4 \pm 0.1$ s^{-1} for wild-type HIV-1 RT (●) and $K_d = 880 \pm 60$ μM and $k_{pol} = 1.6 \pm 0.1$ s^{-1} for AZT^R HIV-1 RT (○).

initiation of (−) strand DNA synthesis by RT, we chose an 18/36-mer primer-template complex as a model substrate for our studies in which the RNA template is identical to the HIV-1 RNA genomic sequence and the primer was complementary to the PBS (Figure 1B). According to the RNA genomic sequence, the first deoxynucleotide triphosphate (dNTP) which will be incorporated is dCTP followed by the second dNTP which is dTTP. We began our studies by examining the time courses for the incorporation of dCMP at the start site using the 18/36-mer RNA/RNA duplex. As shown in Figure 2A, it is clear that there is no difference between the observed first-order rate constants (k_{obsd}) for incorporation of dCMP by wild-type (●) and AZT^R (○) RT (0.97 s^{-1}). The equilibrium dissociation constant (K_d) and maximum rate of polymerization (k_{pol}) values for dCTP for wild-type and AZT^R RT were determined by examining the dependence of k_{obsd} for dCTP incorporation on the concentration of dCTP (Figure 2B). The observation of a weaker affinity of dCTP for RT and its slower rate of incorporation by RT when using an RNA/RNA primer-template substrate as compared to the corresponding DNA/RNA or DNA/DNA substrates is consistent with previous studies (*24*) and studies currently ongoing in our lab.[2] In comparing the kinetic parameters for wild-type (●) and AZT^R (○) RT, we found no significant difference in either the K_d (830 μM) or the k_{pol} (1.5 s^{-1}) values for dCTP. These results demonstrate that wild-type and AZT^R RT are functionally identical with respect to dCTP binding and incorporation at the start site for (−) strand DNA synthesis.

The physiologically relevant reaction to examine AZT resistance in the tRNA^{Lys} initiation step involves the incorporation of dCMP and dTMP or AZTMP. Using the 18/36-mer substrate, we measured the K_d and k_{pol} values for dTTP or AZTTP for wild-type and AZT^R RT in the presence of a saturating concentration of dCTP. Our first indication that there were notable differences in AZT sensitivity between wild-type and AZT^R RT was revealed by gel analysis in examining a time course for the incorporation of a dNTP solution containing dCTP and AZTTP under single enzyme turnover conditions (Figure 3). The incorporation of dCMP forms a 19-mer followed by the incorporation of AZTMP which subsequently forms a 20-mer.[3] As illustrated by the time course in Figure 3A, there is substantial formation (>50%) of 20-mer product for the wild-type enzyme after 3 s. However, for AZT^R RT, there is only a trace of 20-mer formed at 3 s, and the 19-mer band persists even after 20 s because the incorporation of AZTMP is slower (Figure 3B).

It was important to establish that the effects on the kinetics of AZT^R RT were primarily due to changes in the efficiency of incorporation of AZTTP and not that of dTTP. Hence, we compared the time course for the incorporation of dTMP with that of AZTMP (Figure 4). The time courses for the incorporation of dTMP by wild-type (●) and AZT^R (○) RT are identical, occurring with a k_{obsd} of 0.65 s^{-1} (Figure 4A). However, the incorporation of AZTMP by AZT^R RT (○) (0.10 s^{-1}) is 2-fold slower than wild-type RT (●) (0.20 s^{-1}) (Figure 4B). Upon further analysis, the K_d (230 μM) and k_{pol} (0.77 s^{-1}) values for dTTP for wild-type (●) and AZT^R (○) RT were found to be very similar (Figure 5A). However, when comparing AZTTP utilization by wild-type and AZT^R RT, we found approximately a 2-fold change in *both* the K_d and k_{pol} values for AZTTP: $K_d = 160$ μM and $k_{pol} = 0.23$ s^{-1} for wild-type (●) and $K_d = 290$ μM and $k_{pol} = 0.12$ s^{-1} for AZT^R (○) RT (Figure 5B). A complete summary of the kinetic data for dTTP and AZTTP is provided in Table 1. The efficiency of incorporation for dNTP is defined as k_{pol}/K_d and is in general more than 2 orders of magnitude higher

[2] J. A. Vaccaro, H. A. Singh, and K. S. Anderson, manuscript in preparation.

[3] To determine that the rate of AZTMP incorporation was not limited by the rate of dCMP incorporation, a control experiment was performed in which the RT•18/36-mer complex (500 nM RT, 50 nM 18/36-mer) was preincubated for 10 min at 37 °C with saturating concentrations of dCTP (2 mM) and $MgCl_2$ (20 mM) followed by the addition of AZTTP (400 μM). The k_{obsd} values for AZTMP incorporation by wild-type and AZT^R RT were consistent with those determined under conditions in which the RT•18/36-mer complex was *not* preincubated with dCTP and $MgCl_2$.

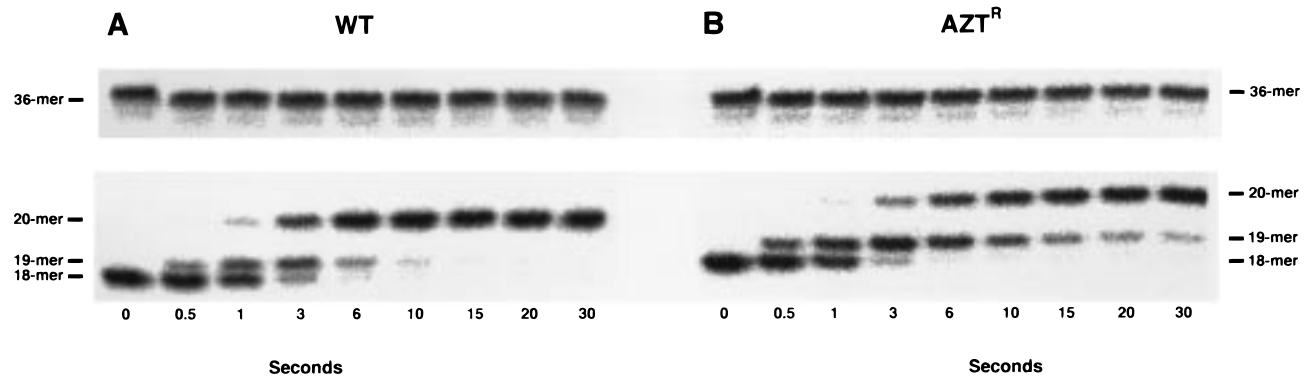

FIGURE 3: Sequencing gel analysis of AZTMP incorporation by HIV-1 RT into 18/36-mer RNA. Wild-type (A) or AZT^R (B) HIV-1 RT (250 nM active sites) and the doubly 5′-^{32}P-labeled 18/36-mer RNA duplex (50 nM) were preincubated on ice for 5 min in buffer [50 mM Tris-HCl (pH 7.8), 50 mM NaCl]. Polymerization was initiated at 37 °C by the rapid addition of 2 mM dCTP and 2 mM AZTTP in buffer containing 10 mM $MgCl_2$, and the reactions were quenched at the indicated times with 0.3 M EDTA as described. Products were analyzed on a 20% polyacrylamide gel containing 7.5 M urea and 12% formamide followed by phosphorimaging analysis. The sizes of the RNA primer (18-mer), the dCMP-extended product (19-mer), the AZTMP-extended product (20-mer), and the RNA template (36-mer) are indicated.

for a DNA/RNA or DNA/DNA substrate as compared with an RNA/RNA substrate (*21*, *30*).[2] The ratio of the efficiency values for incorporation of dTTP versus AZTTP defines the *selectivity* of RT. The selection of dTTP would ultimately result in the successful replication of the 10 000 bp RNA genome whereas AZTTP selection gives rise to chain termination and subsequent cessation of viral replication. A comparison of wild-type RT (2.7) and AZT^R mutant (7.1) selectivity values reveals that the mutant enzyme now has a 2.6-fold higher selectivity for dTTP over AZTTP (Table 1). This difference in selectivity represents the most significant contrast between wild-type and AZT^R RT which has been observed *in vitro* in examining the mechanistic basis of AZT resistance. These results confirm our proposal that changes in the efficiency of AZTTP utilization by RT during RNA-dependent DNA polymerization are involved in the development of AZT resistance (*28*). Furthermore, our present findings extend that proposal by demonstrating that the development of AZT resistance results, in part, from more substantial changes in the selectivity of dTTP versus AZTTP during the initiation phase of reverse transcription when an RNA/RNA primer-template substrate is used to start DNA polymerization. From a structural point of view, these results demonstrate that the decrease in sensitivity of AZT^R RT to AZTTP arises largely from the interaction of AZTTP with an AZT^R RT•RNA/RNA complex rather than with an AZT^R RT•DNA/RNA or AZT^R RT•DNA/DNA complex. This observation implicates the involvement of the structure of the RNA−DNA junction (formed upon attachment of a dNTP to the RNA primer) in the mechanism of AZT resistance.

Although the difference between wild-type and AZT^R RT with an RNA/RNA substrate is significant, the ability to fully account for the 100-fold decrease in the sensitivity to AZT observed in the clinic and in cell culture remains an open question. In thinking about this discrepancy, we have considered the following possibilities:

(1) It has been suggested that even small changes observed *in vitro* in the relative efficiency of incorporation of a chain terminator versus the natural nucleotide will be magnified *in vivo* if one considers the probability of chain termination versus the complete replication of the 10 000 bp RNA genome (*29*, *31*). For example, if the selectivity values in

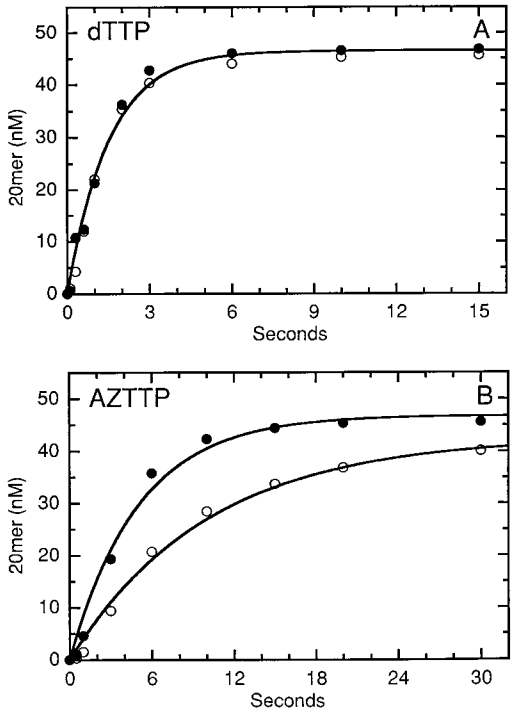

FIGURE 4: Single-turnover kinetics of dTMP or AZTMP incorporation by wild-type and AZT^R HIV-1 RT. (A) The incorporation of dTMP (2 mM dTTP) into the 18/36-mer RNA duplex (50 nM) by wild-type (●) and AZT^R (○) HIV-1 RT (250 nM active sites) was determined at 37 °C in buffer containing 2 mM dCTP and 10 mM $MgCl_2$. The time courses for dTMP incorporation by wild-type and AZT^R HIV-1 RT were fit to a single-exponential equation as described, and the curve is drawn for an amplitude A = 47 nM and an observed first-order rate constant $k_{obsd} = 0.65$ s^{-1} for both wild-type and AZT^R HIV-1 RT. Note that for the purpose of presentation, these values represent an average of the actual individual values: $A = 47 \pm 1$ nM and $k_{obsd} = 0.66 \pm 0.05$ s^{-1} for wild-type (●) and $A = 46 \pm 1$ nM and $k_{obsd} = 0.63 \pm 0.06$ s^{-1} for AZT^R (○) HIV-1 RT. (B) The incorporation of AZTMP (2 mM AZTTP) into the 18/36-mer RNA duplex (50 nM) by wild-type (●) and AZT^R (○) HIV-1 RT (250 nM active sites) was determined at 37 °C in buffer containing 2 mM dCTP and 10 mM $MgCl_2$. The time courses for AZTMP incorporation by wild-type and AZT^R HIV-1 RT were fit to a single-exponential equation as described, and the curves shown represent fits with $A = 47 \pm 2$ nM and $k_{obsd} = 0.20 \pm 0.02$ s^{-1} for wild-type HIV-1 RT (●) and $A = 43 \pm 2$ nM and $k_{obsd} = 0.10 \pm 0.01$ s^{-1} for AZT^R HIV-1 RT (○). Note the difference in scale between panels A and B.

Table 1: Kinetic and Equilibrium Constants for Binding and Incorporation of dTTP or AZTTP by Wild-Type and AZT^R HIV-1 RT

nucleotide	RT	k_{pol} (s^{-1})	K_d (μM)	k_{pol}/K_d (μM^{-1} s^{-1})[b]	selectivity[a,b]
dTTP	WT	0.76 ± 0.04	200 ± 40	$(3.8 \pm 0.8) \times 10^{-3}$	2.7 ± 0.8
AZTTP	WT	0.23 ± 0.01	160 ± 30	$(1.4 \pm 0.3) \times 10^{-3}$	
dTTP	AZT^R	0.78 ± 0.07	270 ± 80	$(2.9 \pm 0.9) \times 10^{-3}$	7.1 ± 2.7
AZTTP	AZT^R	0.12 ± 0.01	290 ± 60	$(4.1 \pm 0.9) \times 10^{-4}$	

[a] Defined as $(k_{pol}/K_d)_{dTTP}/(k_{pol}/K_d)_{AZTTP}$. [b] Errors in the values of k_{pol}/K_d and selectivity were calculated using standard methods (*40*).

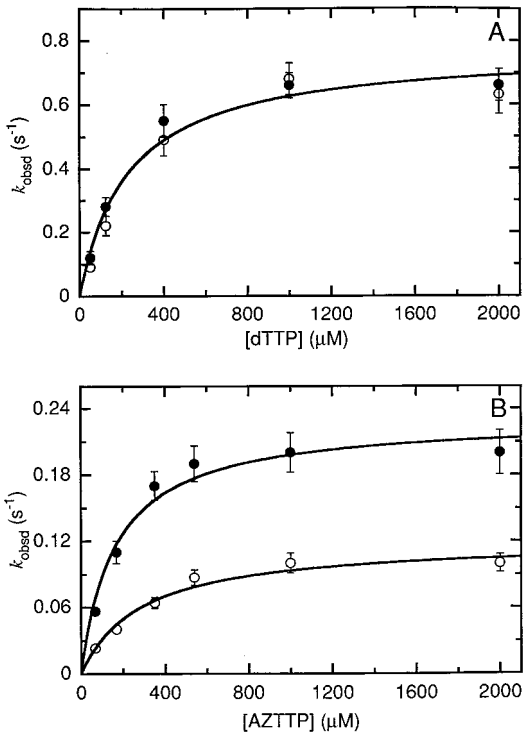

FIGURE 5: Dependence of the observed first-order rate constant k_{obsd} for deoxynucleotide incorporation by wild-type and AZT^R HIV-1 RT on the concentration of dTTP or AZTTP. (A) The dependence of k_{obsd} for incorporation of dTMP into the 18/36-mer RNA duplex (50 nM) by wild-type (●) and AZT^R (○) HIV-1 RT (250 nM active sites) on the concentration of dTTP (50−2000 μM) was determined at 37 °C in buffer containing 2 mM dCTP and 10 mM $MgCl_2$. The dTTP concentration dependence of k_{obsd} for wild-type and AZT^R HIV-1 RT was fit to a hyperbolic equation as described, and the curve shown represents a fit with $K_d = 230$ μM and $k_{pol} = 0.77$ s^{-1} for both wild-type and AZT^R HIV-1 RT. Note that for the purpose of presentation, these values represent an average of the actual individual values that are reported in Table 1. (B) The dependence of k_{obsd} for incorporation of AZTMP into the 18/36-mer RNA duplex (50 nM) by wild-type (●) and AZT^R (○) HIV-1 RT (250 nM active sites) on the concentration of AZTTP (68−2000 μM) was determined at 37 °C in buffer containing 2 mM dCTP and 10 mM $MgCl_2$. The AZTTP concentration dependence of k_{obsd} for wild-type and AZT^R HIV-1 RT was fit to a hyperbolic equation as described, and the curves shown represent fits with $K_d = 160 \pm 30$ μM and $k_{pol} = 0.23 \pm 0.01$ s^{-1} for wild-type HIV-1 RT (●) and $K_d = 290 \pm 60$ μM and $k_{pol} = 0.12 \pm 0.01$ s^{-1} for AZT^R HIV-1 RT (○). Note the difference in scale between panels A and B.

Table 1 are used to calculate the probability of dTMP incorporation at a single site, then there is a 73% chance of incorporating dTMP instead of AZTMP for the wild-type enzyme and a slightly higher chance of 88% for the AZT^R mutant. However, the likelihood of successfully incorporating dTMP at all 39 sites in the U5 and R regions of (−) strand strong-stop DNA (Figure 1A) is approximately 1 in 10^6 for wild-type RT and 1 in 10^3 for the AZT^R mutant.[4] Clearly then it may be possible that a multiplicative effect could lead to larger differences between wild-type and AZT^R RT.

(2) The initiation of (−) strand DNA synthesis *in vivo* involves the human tRNA^{Lys} as a primer annealed to the PBS of the HIV RNA genome. This RNA/RNA duplex is, in fact, a complex structure consisting of intermolecular interactions not only between the tRNA^{Lys} and the PBS but also between the tRNA^{Lys} and sequences flanking the PBS (*32*). For instance, chemical and enzymatic probing studies performed in the absence of RT have shown that the anticodon loop of the tRNA^{Lys} interacts with an A-rich loop of a hairpin structure upstream of the PBS (*33, 34*). Deletion of this A-rich loop from the RNA genomic template results in a reduction in viral replication *in vivo* and decreased (−) strand DNA synthesis *in vitro*, thus providing evidence for the importance of the A-rich loop in HIV-1 reverse transcription (*35*). In addition, template−template interactions have been identified between the two copies of the HIV RNA genome near their 5′ ends (*36*). Since our studies were performed using an RNA/RNA duplex model substrate, even larger differences may be realized upon examination of an RNA/RNA substrate consisting of a full-length tRNA^{Lys} primer and an A-rich loop-containing template that reestablishes the structural features of the true tRNA^{Lys}/HIV genome RNA/RNA duplex.

(3) The decrease in sensitivity of mutant RT to AZT observed in the current study may be augmented *in vivo* by the presence of cellular or other viral factors that are involved in viral replication. One potential factor is the HIV nucleocapsid protein, a small basic Zn^{2+} finger-containing protein that binds to single-stranded regions of RNA (*37*). It has been suggested that the HIV nucleocapsid protein promotes processive polymerization by RT through regions of secondary structure on the HIV genomic template (*38, 39*).

These possibilities are currently under investigation in our laboratory.

In the present study, we have established that the tRNA^{Lys} initiation step plays an important role in understanding the mechanism of AZT resistance. The results outlined here are consistent with previous studies from our laboratory which suggest that the HIV-1 replication events involving an RNA

[4] To a first approximation, the probability of incorporating dTMP at all n independent sites and hence successful chain extension is p^n, where p is the probability of correctly incorporating a single dTMP. For example, the number of thymidines that are required for incorporation in the initiation region of the RNA genome (U5 and R regions) during (−) strand strong-stop DNA synthesis before the first strand-exchange step is $n = 39$. If one assumes the difference in selectivity values for wild-type and AZT^R RT exists at each of the 39 sites, the probability of successful chain completion in the initiation region is 4.5×10^{-6} for wild type [$p = (2.7/3.7) = 0.73$] and 5.9×10^{-3} for AZT^R mutant [$p = (7.1/8.1) = 0.88$], a factor of >1300 favoring chain completion in AZT^R versus wild-type RT. As the number of sites (n) grows, the difference in probable chain completion between wild-type and AZT^R RT clearly increases dramatically.

template are crucial in developing a basic understanding of AZT resistance (*28*). Our current findings, however, extend that proposal by implying that the initiation step is a more critically important and perhaps a more vulnerable stage of reverse transcription than later stages. Consequently, these studies suggest that the tRNA initiation step should be considered in the selection of RT assays to evaluate nucleoside inhibitors as well as in addressing the mechanistic basis of nucleoside drug resistance. A knowledge of the mechanistic aspects of how these mutations imparting AZT resistance allow RT to discriminate between the natural dTTP and the unnatural AZTTP will facilitate the design of better inhibitors.

ACKNOWLEDGMENT

We thank Dr. Stephen Hughes, Dr. Paul Boyer, and Dr. Andrea Ferris for the generous gift of the wild-type and AZT^R RT clones, and Dr. Cathy Joyce, Dr. Janice Pata, and Brad King for technical advice and discussions.

REFERENCES

1. De Clerq, E. (1994) *Biochem. Pharmacol. 47*, 155.
2. Goff, S. P. (1990) *J. Acquired Immune Defic. Syndr. 3*, 817.
3. Mitsuya, H., Yarchoan, R., and Broder, S. (1990) *Science 249*, 1533.
4. Richman, D. D., Rosenthal, A. S., Skoog, M., Eckner, R. J., Chou, T.-C., Sabo, J. P., and Merluzzi, V. J. (1991) *Antimicrob. Agents Chemother. 35*, 305.
5. Yarchoan, R., Mitsuya, H., Myers, C. E., and Broder, S. (1989) *N. Engl. J. Med. 321*, 726.
6. Larder, B. A., Darby, G., and Richman, D. D. (1989) *Science 243*, 1731.
7. Larder, B. A., and Kemp, S. D. (1989) *Science 246*, 1155.
8. Larder, B. A., Kellam, P., and Kemp, S. D. (1991) *AIDS 5*, 137.
9. Larder, B. A. (1994) *J. Gen. Virol. 75*, 951.
10. Kellam, P., Boucher, C. A., and Larder, B. A. (1992) *Proc. Natl. Acad. Sci. U.S.A. 89*, 1934.
11. Kohlstaedt, L. A., Wang, J., Friedman, J. M., Rice, P. A., and Steitz, T. A. (1992) *Science 256*, 1783.
12. Jacobo-Molina, A., Ding, J., Nanni, R. G., Clark, A. D., Jr., Lu, X., Tantillo, C., Williams, R. L., Kamer, G., Ferris, A. L., Clark, P., Hizi, A., Hughes, S. H., and Arnold, E. (1993) *Proc. Natl. Acad. Sci. U.S.A. 90*, 3092.
13. Rodgers, D. W., Gamblin, S. J., Harris, B. A., Ray, S., Culp, J. S., Hellmig, B., Woolf, D. J., Debouck, C., and Harrison, S. C. (1995) *Proc. Natl. Acad. Sci. U.S.A. 92*, 1222.
14. Lacey, S. F., Reardon, J. E., Furfine, E. S., Kunkel, T. A., Bebenek, K., Eckert, K. A., Kemp, S. D., and Larder, B. A. (1992) *J. Biol. Chem. 267*, 15789.
15. Carroll, S. S., Geib, J., Olsen, D. B., Stahlhut, M., Shafer, J. A., and Kuo, L. C. (1994) *Biochemistry 33*, 2113.
16. Caliendo, A., Savara, A., An, D., DeVore, K., Kaplan, J., and D′Aquila, R. (1996) *J. Virol. 70*, 2146.
17. Johnson, K. A. (1986) *Methods Enzymol. 134*, 677.
18. Anderson, K. S., and Johnson, K. A. (1990) *Chem. Rev. 90*, 1131.
19. Johnson, K. A. (1992) *Enzymes* (*3rd Ed.*) *20*, 1.
20. Johnson, K. A. (1995) *Methods Enzymol. 249*, 38.
21. Kati, W. M., Johnson, K. A., Jerva, L. F., and Anderson, K. S. (1992) *J. Biol. Chem. 267*, 25988.
22. Spence, R. A., Kati, W. M., Anderson, K. S., and Johnson, K. A. (1995) *Science 267*, 988.
23. Kerr, S. G., and Anderson, K. S. (1997) *Biochemistry 36*, 14056.
24. Hsieh, J.-C., Zinnen, S., and Modrich, P. (1993) *J. Biol. Chem. 268*, 24607.
25. Reardon, J. E. (1993) *J. Biol. Chem. 268*, 8743.
26. Rittinger, K., Divita, G., and Goody, R. S. (1995) *Proc. Natl. Acad. Sci. U.S.A. 92*, 8046.
27. Johnson, K. A. (1993) *Annu. Rev. Biochem. 62*, 685.
28. Kerr, S. G., and Anderson, K. S. (1997) *Biochemistry 36*, 14064.
29. Krebs, R., Immendorfer, U., Thrall, S., Wohrl, B., and Goody, R. (1997) *Biochemistry 36*, 10292.
30. Lanchy, J.-M., Ehresmann, C., Le Grice, S. F. J., Ehresmann, B., and Marquet, R. (1996) *EMBO J. 15*, 7178.
31. Goody, R. S., Müller, B., and Restle, T. (1991) *FEBS Lett. 291*, 1.
32. Arts, E. J., and Le Grice, S. F. J. (1998) *Prog. Nucleic Acid Res. Mol. Biol. 58*, 339.
33. Isel, C., Marquet, R., Keith, G., Ehresmann, C., and Ehresmann, B. (1993) *J. Biol. Chem. 68*, 25269.
34. Isel, C., Ehresmann, C., Keith, G., Ehresmann, B., and Marquet, R. (1995) *J. Mol. Biol. 247*, 236.
35. Liang, C., Li, X., Rong, L., Inouye, P., Quan, Y., Kleiman, L., and Wainberg, M. A. (1997) *J. Virol. 71*, 5750.
36. Paillart, J. C., Marquet, R., Skripkin, E., Ehresmann, C., and Ehresmann, B. (1996) *Biochimie 78*, 639.
37. You, J. C., and McHenry, C. S. (1993) *J. Biol. Chem. 268*, 16519.
38. Tanchou, V., Gabus, C., Rogemond, V., and Darlix, J.-L. (1995) *J. Mol. Biol. 252*, 563.
39. Ji, X., Klarmann, G., and Preston, B. D. (1996) *Biochemistry 35*, 132.
40. Skoog, D. A. (1985) in *Principles of Instrumental Analysis*, 3rd ed., pp 7−18, Saunders College Publishing, New York.

BI9810353